Fragmentation of fluids by molecular dynamics

S. Toxvaerd
Department of Chemistry, H. C. Ørsted Institute, DK-2100 Copenhagen Ø, Denmark
(Received 8 December 1997; revised manuscript received 11 February 1998)

Fragmentation of fluids is obtained by adiabatic expansions of the volume of systems of Lennard-Jones particles by molecular dynamics simulations. Nontrivial fragmentation is only observed for expansions for which the systems enter the liquid-gas area of the phase diagram. The fragment distribution is established at an early time of the expansions and it is exponential. The expansion regime of fragmentation is demonstrated to depend on the dimension of the system. For a three-dimensional system one only obtains a nontrivial fragmentation for expansion rates for which the late time viscous phase separation growth is suppressed. [S1063-651X(98)01507-4]

PACS number(s): 64.70.−p, 05.70.Ln, 02.70.Ns, 36.40.Ei

I. INTRODUCTION

The interest in fragmentation of fluids by expansions arises from many disciplines in physics and chemistry. The fragmentation is determined by the distribution of fragments, $P(N_{\mathrm{cl}})$ containing N_{cl} mass units. In [1] it is demonstrated that the distribution of galaxies measured by their luminosity, as a measure of the ''big bang'' fragmentation of matter, seems to be exponential. This result has, however, later been questioned by the authors of [2], who suggest that galaxies should follow a log-normal distribution, as many other fragment distributions, obtained in material science. Also in nuclear physics models for fragmentation of fluids play an important role [3]. The present article deals with molecular dynamics (MD) simulations of a fluid that undergoes a process of fragmentation. The fragmentation is ensured by an adiabatic expansion of the volume occupied by the fluid whereby the system breaks up into fragments. The computational setup is described in [1], and is given in the next section. This technique is, however, only one of several computational techniques by which one can obtain a fragmentation. Another procedure applied both computer experimentally [4] as well as in real experiments, is to obtain a fragmentation in a drop of the fluid, e.g., by a local heating of the system or by releasing the pressure instantaneously, in a real experiment by an explosion.

II. ADIABATIC EXPANSIONS OF A FLUID

The MD simulations of adiabatic expansions are performed by expanding the volume with a constant velocity. A system of N particles in a box with volume V_0 and periodical boundaries in all directions are equilibrated to a start temperature, T_0. Then the system is expanded from time, $t=0$, with a constant velocity, $L_0\dot{\eta}$, by expanding the volume in all directions by

$$L_\alpha(t)=L_\alpha(0)(1+\dot{\eta}t), \tag{1}$$

where $L_\alpha(t)$ is the αth box length [in the present simulations the volumes were cubic in three dimensions and quadratic in two dimensions, i.e., $L_0=L_\alpha(0)=V_0^{1/D}$]; $\dot{\eta}$ is the expansion velocity per initial unit length (Hubble constant in cosmological terms). In a laboratory experiment one will, e.g., move a piston (in one direction) in a cylinder and the fluid will respond to this expansion and if the piston is moved sufficiently slowly and with a constant velocity, the system acts as an elastic medium and sets up a linear velocity profile, with a particle mean velocity at the piston that is equal to its velocity and correspondingly a mean velocity at the bottom of the cylinder that is zero. In [1] this steady state velocity profile is also set up at $t=0$ in accordance with the expansion of the volume, by changing all the velocities instantaneously once at the start of the expansion from there values, $\mathbf{v}_i(0)$, to

$$\mathbf{v}_i(0+)=\mathbf{v}_i(0)+\dot{\eta}\mathbf{r}_i(0), \tag{2}$$

where $\mathbf{r}_i(0)$ is the position of the ith particle at $t=0$. This velocity profile ensures a uniform strain at $t=0$ and it is tested (see Sec. III) that the system in a closed, but expanding volume and with no adjustment of the velocities at $t=0$, quickly equilibrates to this expansion setup for small strain rates. Calculations show furthermore that this velocity profile is maintained during the expansion and the setup of the velocity profile thus avoids all initial transients. Finally the periodical boundaries can be taken into account by ensuring that a particle that leaves the box in one direction enters the box from the other side and with a changed velocity accordingly to the expansion velocity of the volume, e.g., if the particle leaves the box at L_α in the αth direction with a positive velocity, $v_\alpha(t)$, it enters the box at its α coordinate equal to zero with a reduced velocity equal to

$$v_\alpha(t+)=v_\alpha(t)-\dot{L}_\alpha(t) \tag{3}$$

and *visa versa*. The last equation ensures a uniformly expansion in an *open* system. (It was, however, also tested that reflecting the particles at the boundaries works equally well). The setup ensures an adiabatic and uniform expansion of the open subsystem with a constant expansion velocity, $L_0\dot{\eta}$, in all directions.

One can immediately predict the physics of the system for the two limit values of the strain rate. For a big expansion velocity and if the particle velocities are not rescaled by Eq. (2) at the start of the expansion, at the initial temperature T_0

and density ρ_0, the particles near the piston cannot diffuse fast enough and the expansion tends to an expansion into a vacuum. In the case where the linear (mean) velocity profile is set up at the start of the expansion the system must be completely fragmentated into its mass units for big strain rates, and on the other hand both kinds of expansions correspond to reversible adiabatic expansions for very small strain rates, so in this case the systems' ''fragmentation'' is given by the systems' equilibrium structure and all the thermodynamic expressions derived for an equilibrium system can be applied provided we have an expression for the systems state variables (e.g., temperature and pressure). But in between these two extremes there might be an interval of strain rates for which a fluid is fragmentated in a nontrivial manner.

In order to determine changes in structure and thermodynamics of the system during the expansion we need expression for the energy, temperature, and pressure during the expansion. The potential energy per particle, u_{pot}, is easily obtained from the instant positions of the particles at time t as usual, and the local velocities, $\mathbf{v}_i'(t)$, are determined as in [1], by subtracting the velocity component due to the expansion

$$\mathbf{v}_i'(t)=\mathbf{v}_i(t)-\dot{\eta}\mathbf{r}_i(t)\frac{L_\alpha(0)}{L_\alpha(t)} \tag{4}$$

from which the ''intrinsic'' temperature $T'(t)$ in the expanding system is calculated. The intrinsic pressure $p'(t)$ is obtained from the intrinsic temperature and the virial of the forces at time t, and the thermodynamic energy per particle $u'(t)$, from $T'(t)$ and $u_{\mathrm{pot}}(t)$, all by applying standard statistical mechanical formulas. This means that one has a measure of when the strain rate is so small that the expansion represents a thermodynamical, reversible path of expansion of the system: Not only must the intrinsic velocities $\mathbf{v}_i'(t)$ be Maxwell distributed, but the particle distribution must also be correct as well as the partition between the two distributions. This is only ensured if the path of expansion goes through equilibrium points, i.e.,

$$p'(t)=p(\rho(t),T'(t)), \tag{5}$$

where $p(\rho(t),T'(t))$ is the equilibrium pressure in a system of particles without any expansion and taken at the temperature $T=T'(t)$ and at the density $N/V=\rho(t)$. According to thermodynamics this criterion of a reversible expansion can equally well be determined as rates of expansion sufficiently small to ensure that

$$u'(t)=u(\rho(t),T'(t)). \tag{6}$$

For strain rates $\dot{\eta}$ bigger than a certain value (depending on the actual instant state point) the expansion is still adiabatic, but irreversible in a thermodynamic sense. Still one can localize a certain barrier of the value of $\dot{\eta}$, which is critical for the expansion: When the initial speed of expansion per unit length $\dot{\eta}$, which introduces local density gradients, exceeds the speed by which local density inhomogeneities are removed, then the system cannot adapt to the expansion, and density gradients are maintained. Although we cannot strictly use equilibrium thermodynamic expressions and relations to determine this critical expansion rate exactly, one will expect that this happens for rates bigger than or of the order of the speed of an adiabatic sound wave. In the present system for values bigger than or of the order

$$\dot{\eta}\approx\sqrt{[\partial p'(0)/\partial\rho(0)]_S} \tag{7}$$

the adiabatic expansion means that L_α increases monotonically with the constant velocity $L_0\dot{\eta}$. At a later time, however, the speed of the expansion *per unit length* is

$$\Gamma_{\mathrm{ex}}=\frac{1}{L_\alpha(t)}\frac{dL_\alpha(t)}{dt}=\frac{\dot{\eta}}{1+\dot{\eta}t} \tag{8}$$

which goes to zero as t goes to infinity. The speed of a sound wave goes to its ideal gas value. So one can see that an eventual fragmentation of a fluid, created at $t=0$ by a supersonic expansion, is not necessarily permanent, since the speed of sound, although getting smaller as the density diminishes, remains finite during the expansion, whereas the speed of the expansion per unit length tends to zero. In other words, a fragmentation, introduced at an early time during the expansion can be removed at a later time. (All expansions end at late time in gas points in the phase space and thus all fragments will evaporate; but this process is slow [6] in three dimensions compared to, e.g., the time it takes to expand from a condensed liquid state to a gas state and thus an established fragmentation can exist for a long time.)

The fragmentation of matter is usually characterized by the distribution $P(N_{\mathrm{cl}})$ of fragments containing N_{cl} mass units. The fragmentation was obtained in Ref. [1] by calculating the cluster distribution $P(N_{\mathrm{cl}})$ at a certain ''late'' time where the mean density was sufficiently low to be able to distinguish between free particles and particles bounded to other particles in a cluster. This method, however, has an element of arbitrariness since one has to specify a certain particle distance, r_{cl} for which a particle belongs to a given cluster, i.e., if the particle is closer than r_{cl} to another particle these two articles are within the same cluster containing N_{cl} particles. Another criterion for pattern in the particle distribution, often used in investigation of, e.g., phase growth, is the structure function, $S(q)$, for small wave number q. This function has no element of arbitrariness and can be used at any time during the expansion. But $Sr(q)$ gives only a coarse-grained information of the actual distribution $P(N_{\mathrm{cl}})$.

The expansion goes through the equilibrium state of the fluid at a sufficiently low expansion rate, and thus a fragment of N_{cl} must explore the phase diagram, i.e., if the temperature $T'(t)$ drops below T_c for mean densities $\rho(t)$, which corresponds to that the system is in the density interval, $[\rho_l,\rho_g]$ of the corresponding liquid and gas, one will have a competition between fragmentation and phase separation. The domain growth of fluid is rather complicated [5] with several growth regimes with different growth laws. The first regime into which the expanded liquid system enters is for $\rho(t)\approx\rho_l$ where (small) vapor drops are created. Spinodal decomposition and growth are observed for densities $\rho\approx\rho_c$ (the critical density). Spinodal growth of domains is characterized by different regimes, with different morphologies and growth speed. Not much, however, is known about the spinodal phase separation of liquid and gas, whereas there have

been many theoretical as well as experiment investigations, including computer experimental investigations of the spinodal decomposition in binary liquid mixtures [7]. Basically, however, the growth and the growth regimes for these two systems should be the same, governed by the same conservation laws, which lead to algebraic growth of the domains with (mean) diameters $R(t)$:

$$R(t) \propto t^n, \tag{9}$$

where n depends on the dimension of the space and the functional form of, and terms in the equation for the growth, i.e., the growth depends only indirectly of the particle potential by the location of a growth regime (and eventually the existence of a growth regime). For viscous growth in 3D, the growth exponent $n=1$ and n is smaller than 1 for all other domain growths in 3D as well as in 2D. If we can use the established result of spinodal growth in binary mixtures for the liquid-vapor separation as well, then we can immediately predict some behavior for fragmentation of fluids in competition with phase growth by spinodal decomposition in the two phase regime: The only phase growth that can resist the homogeneous expansion with constant expansion velocity $L_0\dot{\eta}$ of volume sizes is the viscous growth and only in a 3D space. This follows immediately from comparing the speed of expansion Γ_{ex} with the speed of spinodal growth Γ_{gr} of domains, both taken per unit length. The speed of expansion per unit length is given by Eq. (8), and the speed of an algebraic domain growth of domains with mean diameter $R(t)$ is

$$\Gamma_{gr} = \frac{1}{R(t)} \frac{dR(t)}{dt} = \frac{n}{t}. \tag{10}$$

We consider a nontrivial expansion, i.e., with the presence of phase separation during the (early time of the) expansion. There is a separation growth for

$$\Gamma_{ex} < \Gamma_{gr} \tag{11}$$

but sooner or later the expansion, which asymptotically goes as

$$\Gamma_{ex} \leqslant \frac{1}{t}, \tag{12}$$

will win over all kinds of growth, simply by bringing the system outside all growth regimes and finally outside the density interval of coexisting phases. But the viscous growth in 3D differs from all other growth mechanisms by that, *if* this growth is present it will always exceed the speed of the expansion. This growth, however, is exactly the observed spinodal growth at late times in 3D [8], and so this simple consideration suggests that there might be a fundamental difference between the fragmentation of fluids in 2D and 3D.

III. MOLECULAR DYNAMICS SIMULATIONS OF THE ADIABATIC EXPANSION OF A FLUID

The systems in 2D as well as in 3D all consist of $N=40\,000$ Lennard-Jones (LJ) particles with a potential interaction truncated (and shifted) for particle distances $r_c=2.5\sigma$. The number of particles must be ''rather big'' not only for ensuring good statistics, but also in order to ensure that, e.g., viscous growth can be present during the expansion. (In [8] the viscous regime for phase growth in a binary 3D mixture was observed for growth of domain sizes over a decade of time and using 343 000 LJ-like 3D particles, but for a gas-liquid system the regime might appear at an earlier time and for smaller domain sizes due to the smaller viscosity in the gas-liquid system [5].) The truncation of the potential is also an important detail since the location of the critical temperature T_c is very sensitive to this cutaway of attractions behind r_c. For example, the value of T_c for a 2D LJ system changes from $T_c=0.515$ to $T_c=0.459$ by a cut (and shift) of the potential for $r_c=2.50\sigma$ [9] and the potential used in [1] is for a cut of $r_c=1.74\sigma$ whereby the critical temperature is further lowered; a fact that highly influences the interpretation of the observed results in [1] as will be shown at the end of this section. The gas-liquid phase diagrams for a truncated and shifted Lennard-Jones particles are obtained in [9] (2D) and [10] (3D). The MD (algorithm, etc.) is performed as described in [11], with the additional remark that the time increment h used in the integration algorithm must be taken sufficiently small to integrate accurately for high strain rates. In the preceding all data in the article are given in length units of σ, energy units of ϵ, and time in units of $\sigma\sqrt{m/\epsilon}$, where σ and ϵ are the potential parameters in the Lennard-Jones potential and m is the mass of the particles.

The 3D results are presented first. The system was started with a given $\dot{\eta}$ from an equilibrium point of state at (T_0, V_0), from which the system was left to itself, as described in the previous section. Thus, the expansion can in principle be performed for two different situations. One where the expansion is started from a point of state that corresponds to the system never entering into the region of coexisting (equilibrium) liquid and gas phases during the expansion, and one where the systems mean density, $\rho(t)$, crosses this interval. The results of expansions for which the system does not enter the two-phase part of the phase diagram are first investigated.

The investigation of fragmentation is performed for the adiabatic expansion given by Eqs. (1)–(3), as original used by [1] and later used by several others. The crucial computational setup is Eq. (2) in which one imposes a linear velocity profile at the start of the expansion. It has, however, never been demonstrated that a liquid in a closed volume acts as a viscoelastic medium and quickly equilibrates to a linear velocity distribution when moving the upper walls (piston in a cylinder) with a constant velocity. Furthermore, one could fear that although the fluid does in fact behave as a elastic medium, the fragmentation could be affected be the initial nonlinear expansion, which most take place from the top of the container. In order to investigate the impact of Eq. (2) on the expansion and fragmentation we perform some expansions at different starting state points and for the system expanded by Eqs. (1)–(3) and compared them with expansions by moving the upper walls in a closed container with a constant velocity. The closed system mimics the expansion of a fluid in a closed volumene by moving a piston. The system was, however, expanded in all three directions and the system was surrounded by images so the ''piston'' attracts the

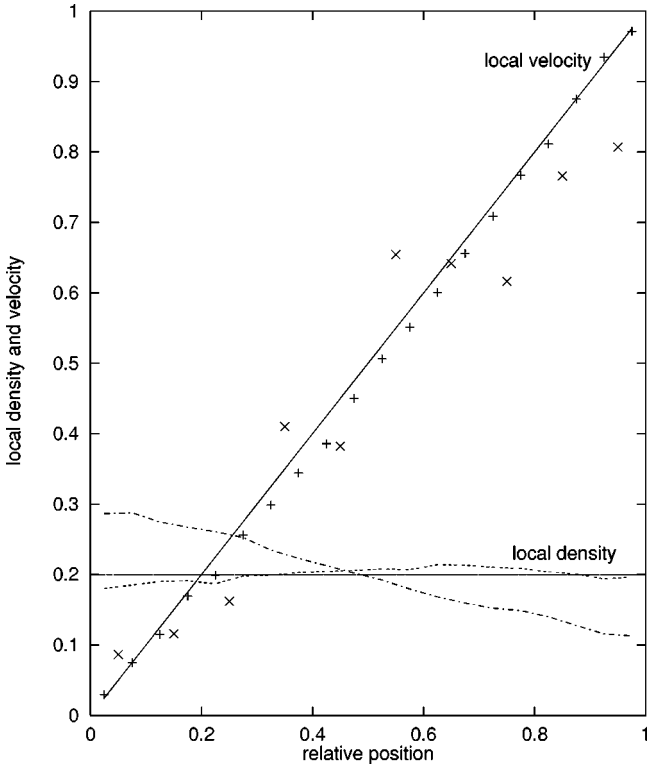

FIG. 1. Local densities $\rho(x)$ (in units of σ^3) and velocities $v(x)$ (in units of the start velocities $L_0\dot{\eta}$), at the end of the expansion, as a function of the position x in the volume (in units of the length of the box). (The mean values are the averages over all three directions.) The lower curves show the density distributions. The dashed line is for a strain rate of $\dot{\eta}=0.05$ and the dash-dotted line is for $\dot{\eta}=0.1$. Also shown with a straight line is the overall mean density $\rho=0.2$. The points show the relative local velocity together with a straight line for a linear velocity profile. (+) is for $\dot{\eta}=0.1$ and (×) is for $\dot{\eta}=0.005$.

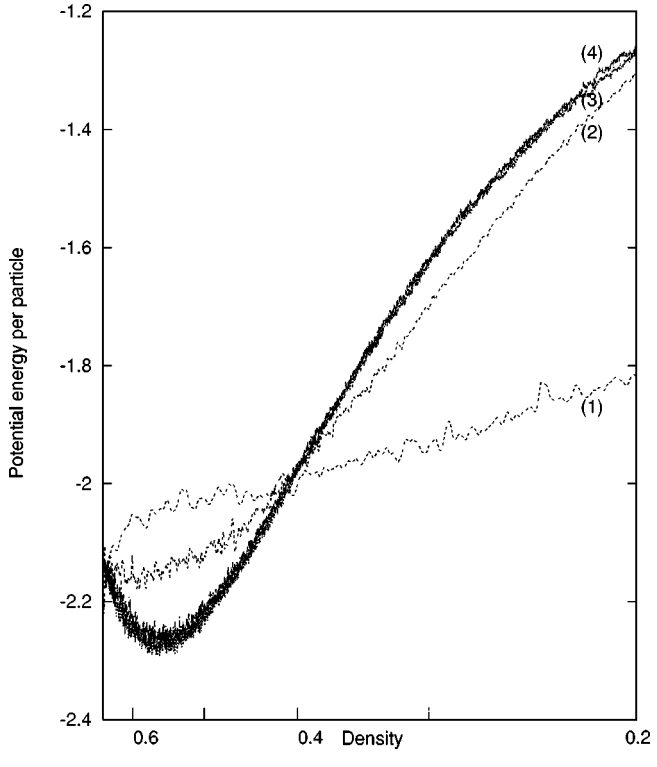

FIG. 2. Potential energy per particle $u_{\rm pot}$ (in units of ϵ/k_B) obtained during the expansions from the particle positions and for different strain rates and as a function of the overall density (in units of σ^3): (1) $\dot{\eta}=0.2$; (2) $\dot{\eta}=0.05$; (3) $\dot{\eta}=0.005$; (4) $\dot{\eta}=0.005$. (1), (2), and (4) are for a closed system without an initial velocity profile. (3) is for an open system and with a initial velocity profile given by Eq. (2).

fluid at $t=0$ by forces identical to the forces across a plane in the uniform fluid at the start of the expansion.

Figure 1 gives the velocity distributions and the density distributions across the container at the end of the expansions. The system was expanded from the state point $(T_0,\rho_0)=(7.5,0.83)$, which corresponds to a liquid point of state at a high temperature (for a noble gas fluid at $T\approx 900$ K). The system was expanded to a volume with the mean density $\rho=0.2$. As can be seen from the figure the system has in fact set up a linear velocity profile and with a uniform density, for velocities of the walls up to $L_0\dot{\eta}=0.05$, and the velocity profile was established during the early time of the expansion. For small expansion velocities we observe, as expected, big fluctuations from the linear profile. For expansion velocities bigger than $L_0\dot{\eta}=0.05$ we still observe a linear velocity profile; but the density distribution is no longer uniform; the viscoelastic medium can no longer respond sufficiently fast to the expansion and the expansion tends to an expansion into a vacuum.

If the expansion is started at $(T_0,\rho_0)=(5,0.65)$, at a less compressed fluid and at at a lower temperature we observe the same behavior, but only for smaller strain values. (The two starting state points are chosen so that the system ends in the same point of state at $\rho_s=0.2$ for a small expansion velocity $\dot{\eta}=0.005$.) Figure 2 gives the potential energy $u_{\rm pot}(t)$ as a function of expansion time for several expansion velocities starting from $(T_0,\rho_0)=(5,0.65)$, together with $u_{\rm pot}(t)$ in an open system and with an initial velocity profile. As can be seen from the figure the time evolutions for the open and closed system agree for $\dot{\eta}=0.005$. For $\dot{\eta}=0.05$ the velocity profile at the end of the expansion is linear, but the density is no longer uniform as was the case when starting from the more compressed fluid, and the potential energy is different from the energy obtained from the slower expansion. The fragment distributions for the open and closed systems, respectively, and obtained from the particle positions at the end of the expansions, show no significant differences.

The conclusion drawn from the two sets of expansions is that if the system is expanded sufficiently rapidly the particles cannot diffuse rapidly enough toward the moving wall at the beginning of the expansion and the expansion continues as an expansion into a vacuum. We have not investigated and determined the fragment distribution for this case of expansions. The ''piston'' velocity barrier for which the viscoelastic fluid cannot respond and where the expansion continues as an expansion into a vacuum is significantly below the sound velocity. Futhermore it is also below the speed by which a single particle in a uniform fluid diffuses [15]. Moving a piston requires a coordinated acceleration and diffusion of particles that apparently lower this barrier significantly. On the other hand, we notice that for a given expansion velocity it is possible to choose a sufficiently compressed

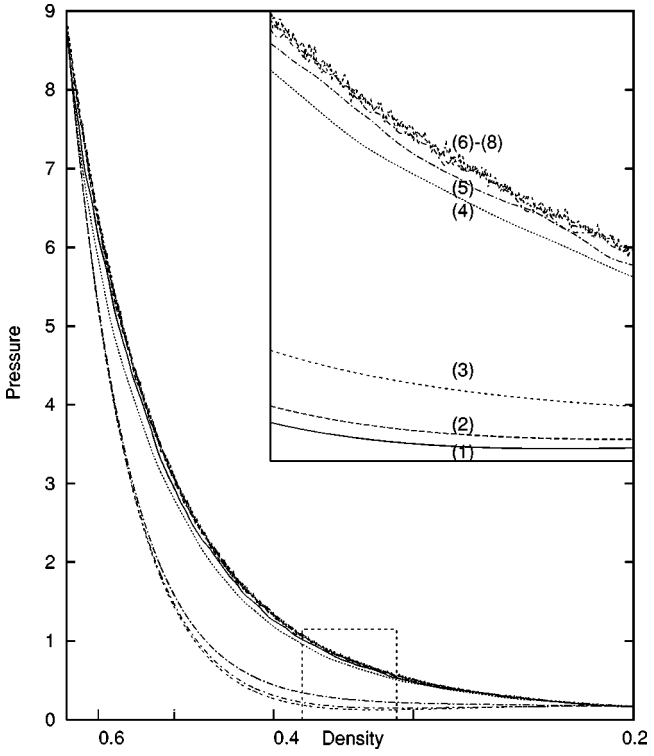

FIG. 3. Intrinsic pressure p' (in units of $\epsilon\sigma^{-3}$) as a function of the density $\rho(t)$ (in units of σ^3) during the adiabatic expansion from $\rho(0)=0.65$ to $\rho(t)=0.20$. The inset shows p' in details in the expansion (density) interval [0.38;0.31]. The various curves are for different expansions rates $\dot{\eta}$: (1) $\dot{\eta}=20$, (2) $\dot{\eta}=10$, (3) $\dot{\eta}=5$, (4) $\dot{\eta}=0.5$, (5) $\dot{\eta}=0.2$; (6)-(8) $\dot{\eta}=0.05$; 0.01 and 0.005, respectively.

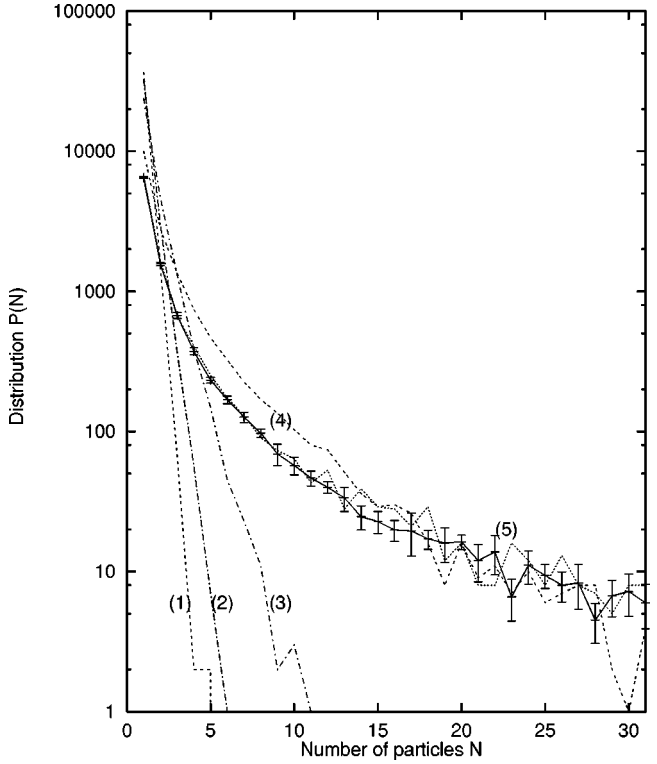

FIG. 4. Distribution $P(N_{\rm cl})$ of ''clusters'' of $N_{\rm cl}$ particles in a fluid at the density $\rho=0.2$. The curve with the full line and uncertainty intervals gives the distribution in a fluid at equilibrium ($\dot{\eta}=0$) where the uncertainty intervals are obtained from ten independent equilibrium configurations. The five other curves are for (1) $\dot{\eta}=20$, (2) $\dot{\eta}=10$, (3) $\dot{\eta}=5$, (4) $\dot{\eta}=1$, and (5) $\dot{\eta}=0.005$.

fluid (point of state) at the start of the expansion for which the linear profile is set up during the early time of the expansion.

The rest of the expansions are performed for an open system given by Eqs. (1)–(3). The first set of expansions is from the point of state $(T_0,\rho_0)=(5,0.65)$ for which the system expands to $\rho_s=0.2$ without entering the two-phase liquid-gas area. At that density all the intrinsic temperatures T' are higher or of the order 1.3 (depending on $\dot{\eta}$). (The critical temperature is $T_c=1.085$). The intrinsic pressures during the expansion for various strengths of strain rates are shown in Fig. 3. The pressures are obtained as functions of expansion times, but compared at equal densities $\rho(t)$. As can be seen from the figure the different functions accumulate into two groups; one that accumulates for small strain rates, and another that accumulates into a limit curve for high strain rates. This behavior is in agreement with the prediction given in the previous section. The square root of the initial slope of the curve for the slow isentropic expansions is 7, and according to the considerations in the previous section one will expect that the system is only ''fragmentated'' for strain rates above, or of the order of, the initial sound velocity, whereas the system should be able to adapt the expansion of the space for rates below this value. (For expansions in closed systems these supersonic and uniform expansions are not possible.)

Figure 4 confirms this result. It shows the $P(N_{\rm cl})$ distributions for $\rho=0.2$ obtained as described in [1] and in the previous section (with $r_{\rm cl}=1.3$, the functional form of the distribution was not sensitive to the value of $r_{\rm cl}$). Also shown in the figure is the corresponding ''fragment distribution'' in an equilibrium system at $(T,\rho)=(1.3,0.2)$ and the uncertainty intervals are from ten independent equilibrium distributions. As can be seen from the figure the distributions nicely confirm the prediction. Only for supersonic initial expansion rates does the fluid fragment, and in very small fragments, whereas the system maintains its equilibrium structure (and intrinsic pressure) for smaller strain rates. But Fig. 4 also shows that the measure of fragment distribution used, $P(N_{\rm cl})$, at the present point of state is misleading, since it indicates that a diluted equilibrium fluid should consist of fragments. It is of course not the case. The distribution, $P(N_{\rm cl})$, only expresses the open fluid structure of a fluid at moderate density. The fragment distributions obtained for the corresponding expansions, but in a closed volumen presented at the beginning of this section (see Figs. 1 and 2) agree nicely with the corresponding distributions for the open system, as expected.

In the second set of experiments the 3D system was expanded from at a point of state, $(T_0,\rho_0)=(1,0.65)$ and with a initial velocity profile (2), from which it enters into the two phase region immediately after the expansion and the expansion was continued until a mean density of $\rho=0.025\approx\rho_g$. At that time, and for a strain rate of $\dot{\eta}=0.2$ the temperature was decreased to 0.60, which, however, is above the triple point temperature for the system so the fragments consist of liquid droplets. The expansions were obtained for strain rates

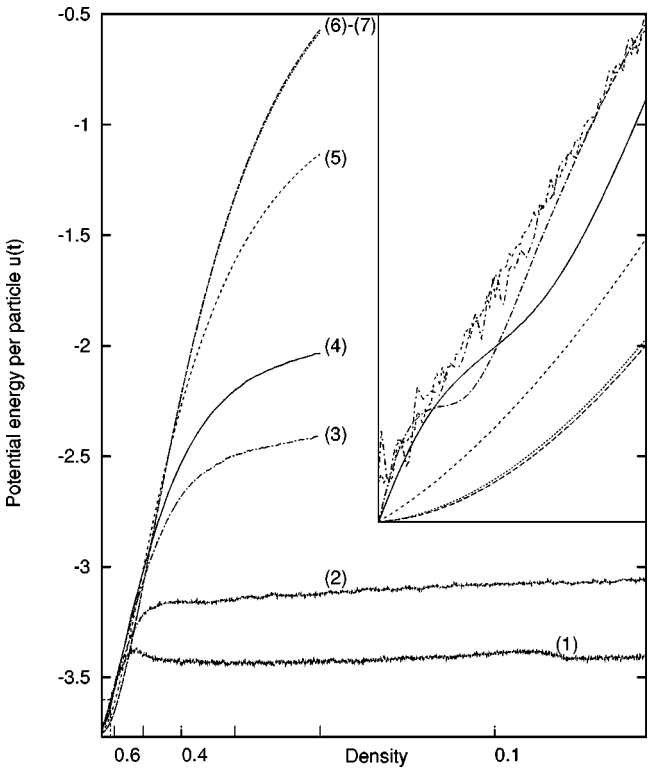

FIG. 5. Potential energy per particle u_{pot} (in units of ϵ/k_B) obtained during the expansions from the particle positions and for different strain rates: (1) $\dot{\eta}=0.001$, (2) $\dot{\eta}=0.01$, (3) $\dot{\eta}=0.1$, (4) $\dot{\eta}=0.2$, (5) $\dot{\eta}=1$; (6) $\dot{\eta}=10$ (dots), and (7) $\dot{\eta}=20$. The inset shows $u_{\mathrm{pot}}(t)$ at the start of the expansion for $\rho(t)\in[0.65,0.61]$.

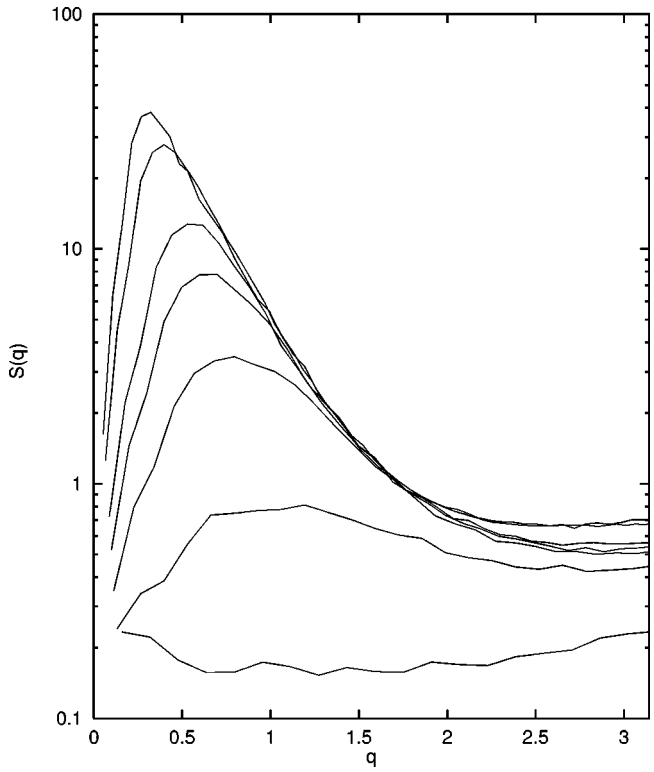

FIG. 6. The structure function $S(q)$ for q less than π. The functions are obtained from positions at various times during the expansion with $\dot{\eta}=0.2$. The lower curve is the S(k) for the starting positions at $T=1.2$ and $\rho=0.65$ and the six succeeding curves are obtained during the expansion at the densities $\rho(t)=0.38$, 0.24, 0.16, 0.11, 0.05, and 0.025, respectively.

in the interval $\dot{\eta}\in[0.001,20]$, and the calculations confirm the prediction that the system fragmented completely for very fast expansions. For very slow expansions, however, the system separates into a two-phase system of one liquid phase and one gas phase; but in between these two trivial limits there is a big interval of strain rates for which the fluid was fragmented. A series of observations demonstrate this fact. Figure 5 shows the potential energy $u_{\mathrm{pot}}(\rho(t))$ during the expansions and the inset gives the variations at the beginning of the expansions. The potential energies fluctuate with (expansion) times for small strain rates as in an equilibrium system, but their mean values agree and indicate that the system is expanded thermodynamically in a reversible manner. The potential energies also agree for different but very fast expansions and over almost the whole density region, but in between these limits there is a big interval of strain rates for which the system ended in widely different potential energies. This is due to differences in the fragmentation. From the inset it can be seen that the variations in $u_{\mathrm{pot}}(\rho(t))$ at very early times, and for the intermediate strain values $\dot{\eta}=0.2$ and 0.1, exhibit a looplike form, which indicates that the onset of fragmentation starts at very early times as also found by [3] (for a 2D system).

The strain rate $\dot{\eta}=0.2$ was chosen for special investigation since it is in between the two extreme values of expansion rate, and with a fragment distribution with a maximum cluster of the order a few hundred particles, which ensures the best statistics. For an expansion in a closed system and without setting up the linear velocity profile, the system must be compressed to a much higher density than $\rho=0.65$ at the start of the expansion in order that the fluid can establish the profile before entering the two phase area. The dynamics of fragmentation can be investigated by obtaining the structure function, $S(q)$, during the expansion. Figure 6 shows $S(q)$ for various times (mean densities) during the expansion and for a strain rate of $\dot{\eta}=0.2$. The structure function for q values smaller than π gives a coarse-grained indication of the dynamics of fragmentation and the distribution of e fragments. As can be seen from the figure the fragmentation certainly appears at an early time of the expansion, as one would expect. One can also see from the location of the maximum of the peak, which has not shifted very much toward smaller q values during late time of the expansion, that the mean size of the fragments only increases a little during the last part of the expansion. One would expect that the created clusters grow, at least for sizes bigger than the critical droplet size for droplets in the nucleation region, but from $S(q)$ [and the first moment of $S(q)$] it was estimated that the growth of the clusters was suppressed by the expansion. This fact is, however, much more clearly seen from the fragment distribution $P(N_{\mathrm{cl}})$, obtained during the late stage of the expansion. At the diluted densities ($\rho=0.05$ and 0.025) the clusters are found to be well separated (so the distributions do not depend on the choice of r_{cl}, which was set to 1.5σ). Figure 7 gives the distribution of fragments for $\dot{\eta}=0.2$. The full line and uncertainty intervals are the mean of ten independent expansions from T_0,ρ_0 configurations to

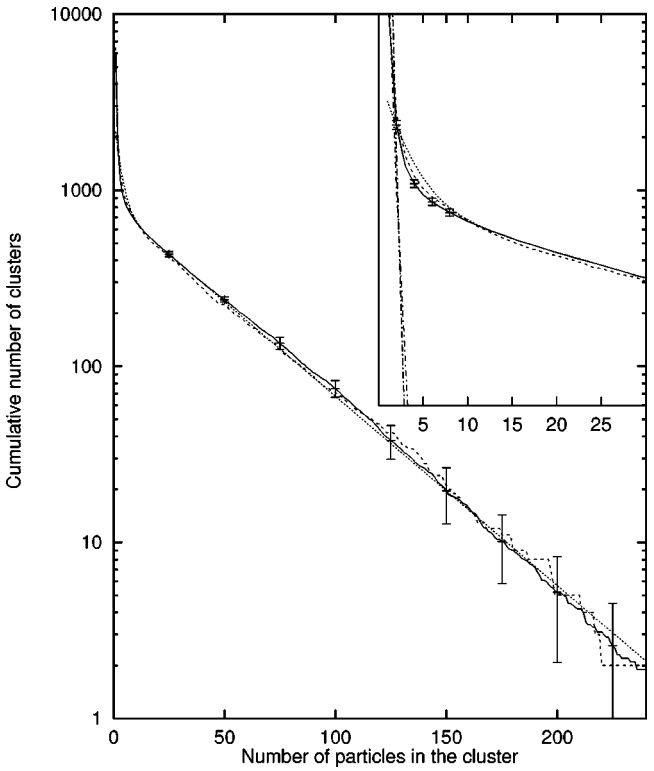

FIG. 7. Cluster distributions in a 3D fluid. The full line and uncertainty intervals is for the fluid expanded with $\dot{\eta}=0.2$ to a mean density of $\rho=0.025$ and the uncertainties are obtained from 10 expansions with different (equilibrium) start configurations. The bimodal distribution is shown by dots and the dashed curve is the distribution of one (representative) of the ten expansions, but taken at the intermediate density $\rho=0.05$. The inset shows the distributions up to cluster size 30, and the two curves (dashed-dotted line) also shown in the inset are the distributions obtained for a $\dot{\eta}=5$ and the gas distribution for $\dot{\eta}=0.001$.

the mean density $\rho=0.025$ and it gives the accumulated cluster distribution. The biggest cluster observed in the ten expansions consists of 377 particles; and the logarithmic plot demonstrates that a bimodal exponential distribution (dots) describes the distribution within the accuracy of the data over several decades of $P(N_{\mathrm{cl}})$.

Also shown in the figure (dashed line) is the distribution at the density $\rho=0.05$ of one (representative) of the ten systems expanded, from which it is clearly seen that the distribution is not changed at late times. The inset, which also shows the gaslike distribution (dot-dashed line) for big expansion rates, demonstrates, however, that the bimodal distribution does not describe the distribution of small droplet perfectly.

The droplets get bigger for smaller strain rates than $\dot{\eta}=0.2$, and the domain structure of the fluid, for a strain rate of $\dot{\eta}\approx 0.01$, looks like the structures obtained by spinodal decompositions of binary mixtures where both phases extend through the whole volume. As pointed out in the previous section, if in 3D one gets to a structure during the expansion that contains viscous growth, then this growth will remain in the system until the system is brought outside this growth domain. Furthermore, the domains percolate the volume for spinodal decompositions in binary mixtures at $\rho\approx\rho_{\mathrm{cr}}$. Since

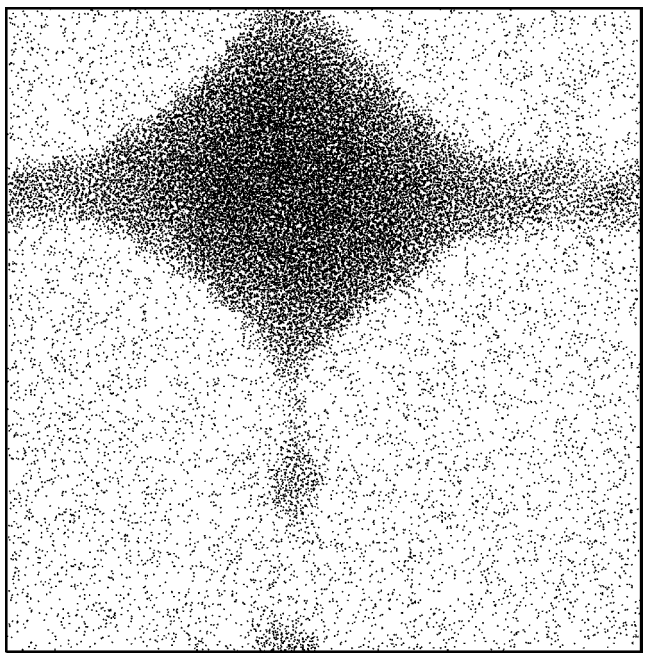

FIG. 8. Projection of the particle distribution (x_i,z_i) in a 3D fluid, the two other 2D projections are similar. The particle distribution is obtained for a very slow expansion rate of $\dot{\eta}=0.001$ and the figure shows the distribution at the mean density $\rho=0.05$ at the time where the liquid stops percolating the 3D space.

the expanded system necessarily must cross this density zone during the expansion one will *a priori* expect the same to happen in this system. For example, for sufficiently small strain rates, one will expect the system to break up into subphases of gas and liquid, which both percolate the volume in all directions (''plummer's nightmare''). With this fact in mind it is possible to be more precise about the statement on when the expansion brought the system outside the region of viscous growth: It happens when the system of the liquid, which percolates the volume in all three directions, breaks up. To test this hypothesis, the system was expanded with a very small strain rate of $\dot{\eta}=0.001$ and one observed exactly the behavior described above. Figures 8 and 9 show the projections of the positions at the time where they just no longer percolate the volume (Fig. 8) and the particle distribution at the end of the expansion at $\rho=0.025$ (Fig. 9), where the system has ended in one big liquid drop of 29 272 particles surrounded by 10 728 gas particles with a gas distribution shown in the inset of Fig. 7. Since it has not been the aim of the present investigation to determine spinodal phase growth in a quenched liquid-gas system the expansions at small strain rates have only been used to estimate the limit strain for that a fragmentation is maintained. The limit value of strain which gives a fragmentation is the strain rates for which the fluid, by passing the spinodal growth regime during the expansion, does not percolate the volume.

Finally a system of 40 000 LJ particles, but in 2D, was expanded and in the first set of expansions through one-phase fluid points in the phase diagram down to a density of $\rho=0.2$ and temperature $T=0.55$ above the critical temperature [9], $T_{\mathrm{cr}}=0.459$ for the corresponding equilibrium system. The ''cluster distribution'' at the end of the expansion for a density of $\rho=0.2$ is given in Fig. 10. As can be seen

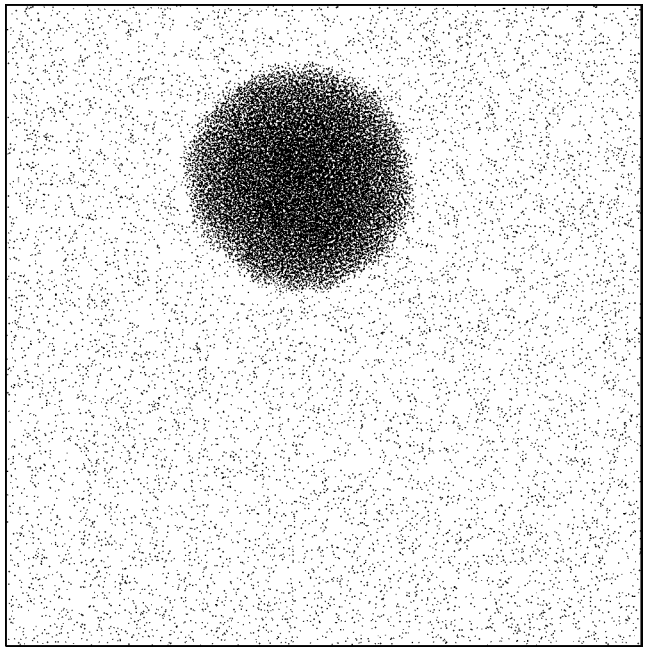

FIG. 9. Projection of the particle distribution (x_i, z_i) for the same system as shown in Fig. 8; but at the density $\rho = 0.025$.

from the figure the distributions are bimodal, as observed in [1]. But so is the equilibrium ''cluster distribution'' in a 2D system at the same temperature and density, and from the figure one can see that the bimodal distribution, also obtained by [1], is isomorphic with the equilibrium structure.

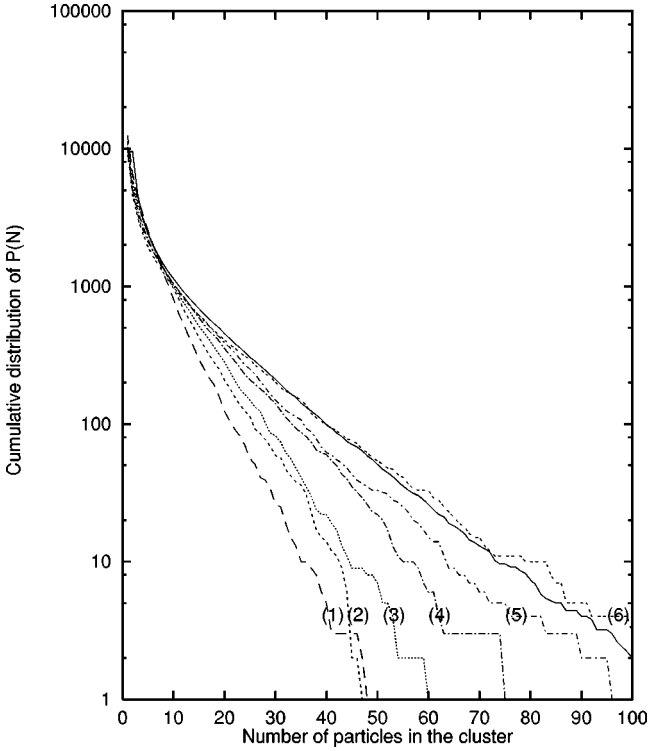

FIG. 10. Cumulative distribution of $P(N_{\mathrm{cl}})$ for a 2D LJ system at $\rho = 0.2$. With the full line is the mean of the distribution obtained from five different equilibrium distributions at the same temperature and density. The other distributions are for (1) $\dot{\eta} = 0.2$, (2) $\dot{\eta} = 0.1$, (3) $\dot{\eta} = 0.05$, (4) $\dot{\eta} = 0.025$, (5) $\dot{\eta} = 0.01$, and (6) $\dot{\eta} = 0.005$.

Thus the distribution function $P(N_{\mathrm{cl}})$ gives a misleading picture of the structure in moderate dense fluids at $\rho \approx 0.2$ both in 2D as well as in 3D (Fig. 4). The 2D result differs, however, from the corresponding 3D result, shown in Fig. 4, in that the nonequilibrium structures converge more slowly toward the equilibrium distribution as the expansion rate goes to zero. The ''fragmentations,'' shown in Fig. 10, measured by their difference from the equilibrium distribution are, however, not stable but disappear (slowly) as the expansions are continued.

The potential in [1] was, as mentioned above cut at $r_c = 1.74$ (but not truncated [12]) so the phase diagram referred to in [1] is irrelevant and the phase diagram for the potential used in [1] is not known. In order to estimate the importance of the different cut we calculated the potential energy per particle in the fluid state $(T, \rho) = (0.60, 0.65)$, used later.

The potential energy is

$$u_{\mathrm{pot}} = \frac{1}{2} \int_0^\infty d\mathbf{r} g(r) r \rho u_{\mathrm{LJ}}(r), \tag{13}$$

where $g(r)$ is the radial distribution function, and this is the relevant quantity to consider, when cutting away potential energy. In the present computation the potential is cut at $r_c = 2.5\sigma$ and shifted by $u_{\mathrm{LJ}}(r_c)$. In [1] the potential is spline fitted to go to zero in the interval $r \in [1.24, 1.74]$ whereby a particle almost only interacts with its five to six nearest neighbors, but with a full LJ potential. The potential energy for a LJ system without any cut and at $(T, \rho) = (0.60, 0.65)$ was calculated to be $u_{\mathrm{pot}} = -1.947$ and the potential energy for a truncated $(r_c = 2.5)$ and shifted potential was -1.797 and it is this reduction of the binding energy that lowers the critical temperature by about 10%. The spline fitted potential used in [1] gives a potential energy, $u_{\mathrm{pot}} = -1.619$; at that point of state and from the figure caption to Fig. 5 in [1] one can see that their temperature at $\rho = 0.175$ is $T = 0.39$ and their expansions *cannot* be within the two-phase area. This is the reason for the ramified ''clusters'' obtained in [1], which in fact is isomorphic with the (supercritical) equilibrium structure in the 2D fluid.

The 2D system was finally expanded through liquid-gas points of state in order to investigate the hypothesis that the fragmentation at an adiabatic expansion differs in 2D and 3D. The system was started at $(T, \rho) = (0.60, 0.65)$ and it entered the two-phase region shortly after the expansion, which was continued until a density $\rho = 0.026 \approx \rho_g$. Figure 11 gives the particle distribution for a very slow expansion rate of $\dot{\eta} = 0.001$, and it demonstrates that the spinodal growth [13,14] has not been able to compete with the expansion to the same degree as in 3D. For faster expansion rates (than $\dot{\eta} = 0.001$) the system ends in stable, exponentially distributed fragmentated states, but with smaller fragments than for a corresponding 3D expansion.

IV. CONCLUSION

Computer simulations of expansions of fluids can be performed in many ways. If the system is expanded with a constant velocity (well below the speed of sound) from a compressed state, then the fluid acts quickly as a viscoelastic

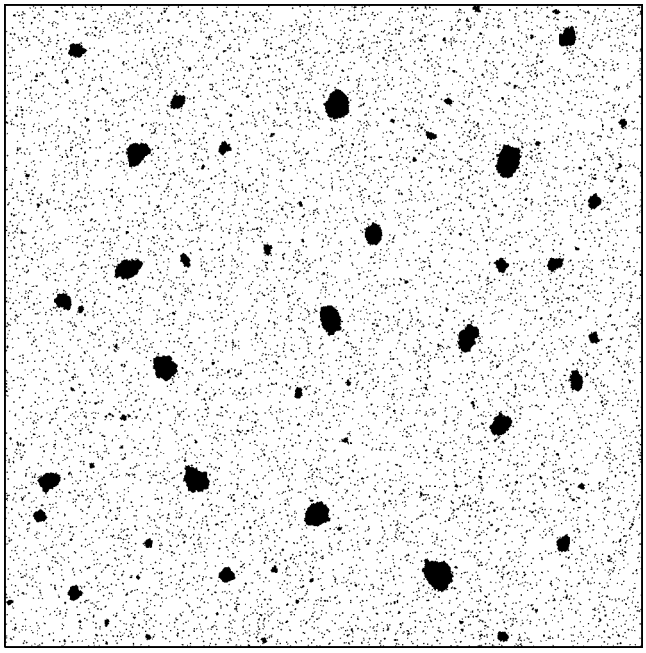

FIG. 11. Particle distribution in a 2D system at $(T,\rho)=(0.3,0.026)$ after a very slow expansion rate of $\dot{\eta}=0.001$.

medium and sets up a linear velocity profile in the container and the fluid expands uniformly. This kind of uniform expansion is investigated by molecular dynamics simulations. The computer experiments demonstrate that the equilibrium phase behavior plays a crucial role for a stable fragmentation of the fluid. The fragmentation at state points above the two-phase region (Fig. 4), is only obtained for very fast expansion rates and disappears (slowly) as the expansions are continued. This is explained by the fact that a constant expansion rate of the sizes implies that the speed of the expansion per unit length goes to zero whereas the capability of removing a density inhomogeneity is given by the sound velocity, which remains finite. Thus a fragmentation that is obtained at an early time of the expansion, e.g., by an explosion, disappears at a later time.

The adiabatic expansion is associated with a strong decrease in temperature and the fragmentation competes with phase growth, including spinodal phase growth, if the system enters into the liquid gas area of the phase diagram. A three-dimensional system differs significantly from a corresponding two-dimensional system in several ways. In 3D the two phases can percolate the volume in all directions at the same time (''plummer's nightmare'') whereas a phase percolation in 2D is a frontier and obstacle for the other phase. Furthermore the spinodal phase growth has a smaller exponent for the algebraic growth speed in 2D than in 3D, where the viscous growth is the only growth that can compete with the expansion. This growth is, however, the observed spinodal growth in 3D at late time [8], and the very slow expansions in 2D and 3D confirm this difference (Figs. 8, 9, and 11). For a slow expansion the system separates into a big drop of liquid surrounded by its gas; whereas there is an interval of bigger expansion rates for which the system is fragmentated when leaving the two-phase area. The fragment sizes are *exponentially* distributed.

The fragmentation by a uniform expansion of a (2D) Lennard-Jones fluid was in [1] compared with the luminosity of galaxies as a measure of the big bang fragmentation of matter. According to [1] this is also exponentially distributed; but later this result was questioned since if matter in the Universe is fractally distributed one should in fact expect an algebraic distribution [16] rather than an exponential distribution. The fragments in the present LJ system, without long range gravitational forces, are exponentially distributed and different from the droplet distribution for growth outside the spinodal percolating regime [17]. The mean of ten expansions, which gives the uncertainty of the distribution, clearly shows an exponential distribution over several decades (Fig. 7); but it is of course a question whether there exists that kind of universality between fragmentation of obstacles with widely different forces. Perhaps one important result from the present investigation might be helpful in this context: one observes that the distribution of fragments is established at an rather early times during the expansion, as demonstrated in Fig. 7, and thus the distribution of matter in the Universe should be independent of the age of the galaxies.

[1] B. L. Holian and D. E. Grady, Phys. Rev. Lett. **60**, 1355 (1988).

[2] L. Baker, A. J. Giancola, and F. Allahdadi, J. Appl. Phys. **72**, 2724 (1992).

[3] A. Strachan and C. O. Dorso, Phys. Rev. C **55**, 775 (1997), and articles quoted therein.

[4] J. A. Blink and W. G. Hoover, Phys. Rev. A **32**, 1027 (1985).

[5] A. J. Bray, Adv. Phys. **43**, 357 (1994).

[6] K. Yasuaka, M. Matsumoto, and Y. Kataoka, J. Chem. Phys. **101**, 7904 (1994).

[7] See, e.g., the previous reference and J. D. Gunton, M. San Miguel, and P. S. Sahni, in *Phase Transitions and Critical Phenomena*, edited by C. Domb and J. L. Lebowitz (Academic Press, New York, 1983), Vol. 8, p. 265 and references therein.

[8] M. Laradji, S. Toxvaerd, and O. G. Mouritsen, Phys. Rev. Lett. **77**, 2253 (1996).

[9] B. Smit and D. Frenkel, J. Chem. Phys. **94**, 5663 (1991).

[10] B. Smit and D. Frenkel, J. Chem. Phys. **96**, 8639 (1992).

[11] S. Toxvaerd, Mol. Phys. **72**, 159 (1991); Phys. Rev. E **50**, 2271 (1994).

[12] B. L. Holian and D. J. Evans, J. Chem. Phys. **78**, 5147 (1983).

[13] E. Velasco and S. Toxvaerd, Phys. Rev. Lett. **71**, 388 (1993); Phys. Rev. E **54**, 605 (1996).

[14] S. Toxvaerd, Phys. Rev. E **53**, 3710 (1996).

[15] D. Levesque and L. Verlet, Phys. Rev. A **2**, 2514 (1970). When using their Eq. (49) one has to multiply with a factor of $\sqrt{48}$ due to a different time unit in the reference.

[16] See M. Montuori, F. Sylos Labini, and A. Amici, Physica A **246**, 1 (1997), and references therein.

[17] T. M. Rogers and R. C. Desai, Phys. Rev. B **39**, 11 956 (1989).